

## CHAPTER V

### OPTICAL AND X-RAY STUDIES OF THE TWISTED SMECTIC C AND TWISTED NEMATIC PHASES

#### 1. Introduction

**Smectic C** may be described as a tilted form of **smectic A**: the molecular centres are arranged at random in a liquid like fashion within each layer, as in **smectic A**, but the preferred molecular axis is tilted with respect to the layer normal. In certain compounds (e.g., p-n-heptyloxyaeoxybeneene) the tilt angle (measured with respect to the layer normal) is practically independent of temperature, but if the **smectic C** phase is followed by **smectic A** at a higher temperature [e.g., terephthal-bis(-p-butylaniline)], the tilt angle decreases with temperature becoming zero at <sup>the</sup> 0-A transition point. **Smectic C** is optically biaxial; the optic axial angle is normally quite small ( $\sim 10^\circ$ ) and is practically temperature independent. **Saupe** (1969) pointed out that **smectic C** bears

some similarities with the nematic in regard to its elastic properties and that there should therefore exist a twisted form of this structure resembling the twisted nematic or cholesteric phase. Subsequent studies (Leclercq et al. 1969, Arora et al. 1970, Helfrich and Oh 1971) have established the occurrence of the twisted smectic C modification in mixtures as well as in pure compounds. Berreman (1972) has shown theoretically that single domain samples of cholesteric and twisted smectic C phases have identical optical properties for light incident in the direction of the axis of twist. In this geometry, a single Bragg-reflection band at  $\lambda = \mu P$  exists for either type of liquid crystal. However, with obliquely incident light the twisted smectic C sample would show an additional Bragg-reflection band at  $\lambda = 2\mu P$ . In his calculations he assumed the local order in smectic C as uniaxial whereas in reality it is weakly biaxial (Taylor et al. 1970). The differences between TSC structure and the classical cholesteric structure are given in table 1.

Table 1

<u>Twisted smectic C</u>	<u>Cholesteric</u>
1) Molecules are arranged in well defined layers.	There is no such layering.
2) Molecules are tilted at an angle to the helical axis.	Molecules are normal to the helical axis.
3) The local order is optically biaxial.	The local order is optically uniaxial.
4) This phase can have another mesophase at higher temperatures.	This phase directly goes over to the isotropic phase.

The optical rotatory power of a TSC phase and a cholesteric phase for a few wavelengths as a function of thickness has been reported by Helfrich and Oh. Their measurements were carried out on bis-(p-6-methyl octyloxy-benzylidene)-2-chloro-1,4-phenylene diamine which exhibits two mesophases, a TSC phase and a cholesteric phase, separated by a first order phase transition. One noteworthy property which they find in their TSC system is the absence of any measurable temperature effect on optical rotation unlike in the cholesteric phase where the optical rotation is strongly dependent on temperature. Brunet (1975) found that bis-(4'-n-decyloxy benzal)2-chloro-1-4-phenylene diamine (DOBCP) containing 5% cholesteryl cinnamate (which shows both the TSC and TN phases) exhibits an optical rotation which is strongly dependent on temperature in both mesophases. These experimental results are presented in Figure 1. The optical rotatory power (measured for  $0.5893 \mu\text{m}$ ) decreases with increase in temperature with a very weak jump at the transition temperature. The rate of decrease

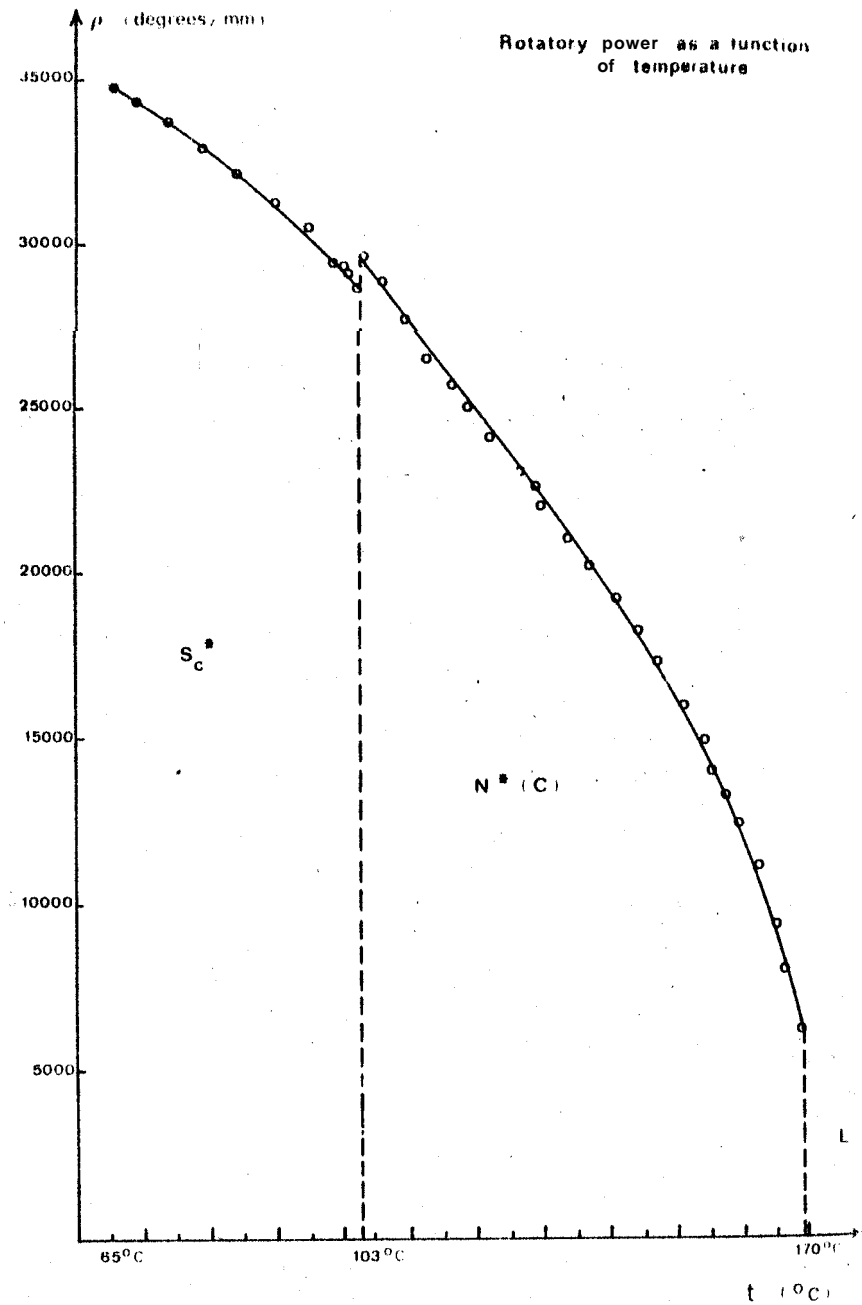


Figure 1: Rotatory power as a function of temperature for the sodium D line in the twisted smectic C and in the twisted nematic phase (Brunet 1975).

is higher in the TB phase compared to that of the TSC phase.

This chapter presents detailed optical studies on the TSC and TN phases of a mixture of 4,4'-di-n-heptyloxy azoxybenzene (HOAB) and cholesteryl benzoate (CB) for two compositions (0.9 HOAB + 0.1 CB and 0.85 HOAB + 0.15 CB). The optical rotatory power  $\rho$  and pitch  $P$  measured as functions of temperature change discontinuously at the TSC-TN phase transition, the values being higher in the lower temperature phase. The birefringence  $\Delta \mu$  of pure HOAB has also been determined in the nematic and smectic phases. An attempt has been made to account for the experimental results in terms of the theory of light propagation in cholesterics. It is found that the observed  $\rho$  in the TN phase cannot be accounted for in terms of the measured values of  $\Delta \mu$  and  $P$ . The calculated value is too high indicating that, in contrast to the classical cholesteric structure, the molecules in this phase are not normal but inclined with respect to the

helical axis. This molecular tilt has been confirmed by X-ray studies,

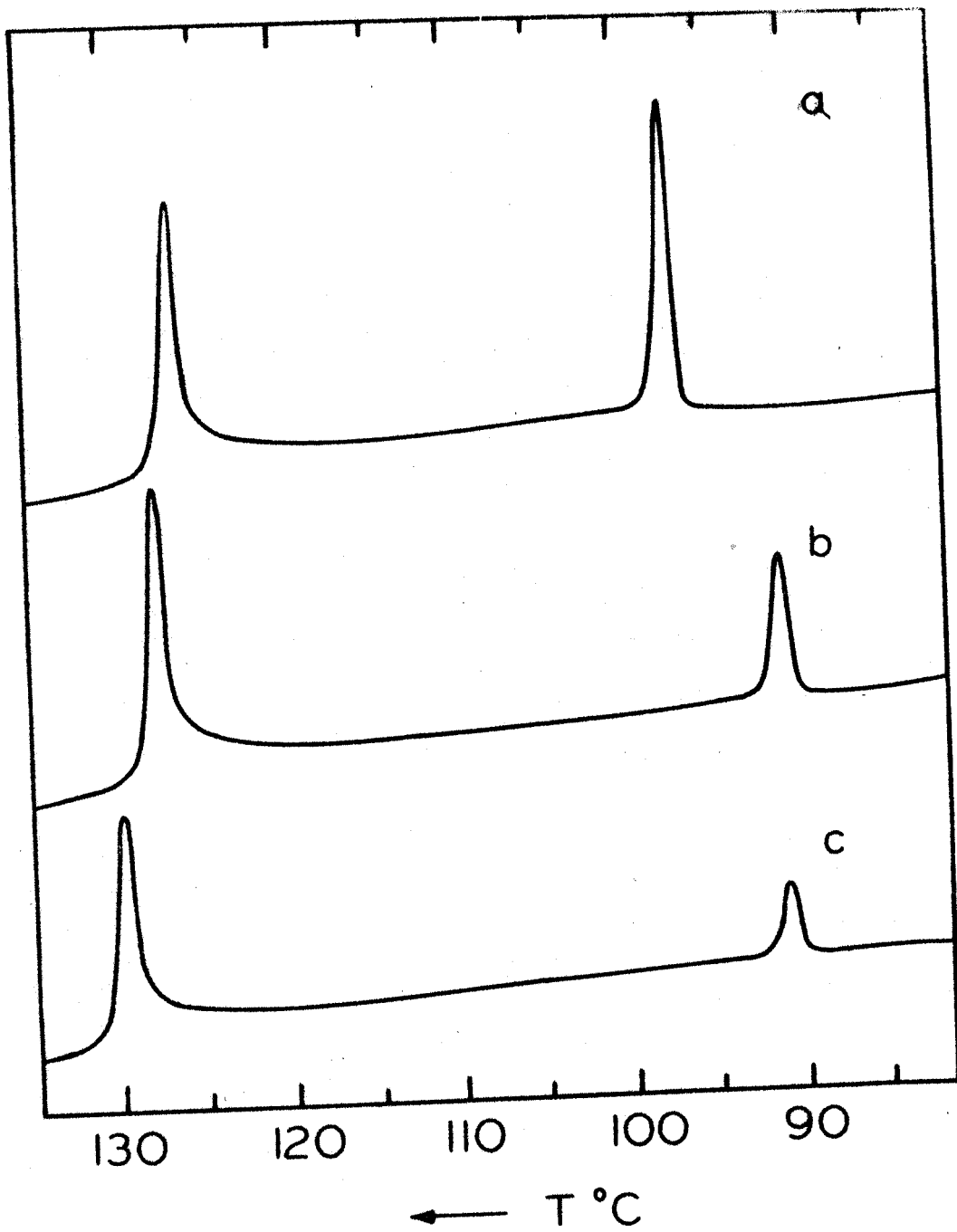
## 2. Experimental measurements

The compounds used in these experiments were HOAB obtained from Eastman Kodak Company (U.S.A.) and cholesteryl benzoate obtained from Vari-Light Corporation (U.S.A.), HOAB adopts a tilted smectic C phase at lower temperatures and nematic phase at higher temperatures. The differential scanning calorimetric (DSC) trace, taken with a Perkin-Elmer DSC-2 (U.S.A.) instrument, of HOAB showing the smectic C-nematic and nematic-isotropic transitions are given in Figure 2a. Cholesteryl benzoate adopts only <sup>one mesophase, viz., the</sup> cholesteric phase. Its transition temperatures are as follows:



The mixtures were prepared by taking the

**Figure 2: Differential scanning calorimeter traces showing (a) the smectic C-nematic and nematic-isotropic transitions for HOAB, (b) & (c) the twisted smectic C-twisted nematic and twisted nematic-isotropic transitions for the 0.9 HOAB + 0.1 CB and 0.85 HOAB + 0.15 CB mixtures respectively.**



compounds in the required ratio in a glass cup and heating it to isotropic phase. In the isotropic phase it was stirred well and then cooled to liquid crystalline phase. The DSC traces of the 0.9 HOAB + 0.1 CB and 0.85 HOAB + 0.15 CB mixtures taken under similar conditions are given in Figures 2b and 20 respectively. The traces show that in each mixture the two mesophases are separated by a first order phase transition. Apart from changes in the peak heights, the traces are similar to the one found in pure HOAB. This indicates that addition of CB does not have a very much effect on the helical structure, i.e., nematic like in the higher temperature phase and smectic like in the lower temperature phase. It was found that both phases exhibit optical rotation. These properties indicate that the higher temperature mesophase is twisted nematic (TN) and lower temperature mesophase is twisted smectic C (TSC) phase.

#### Optical rotatory power

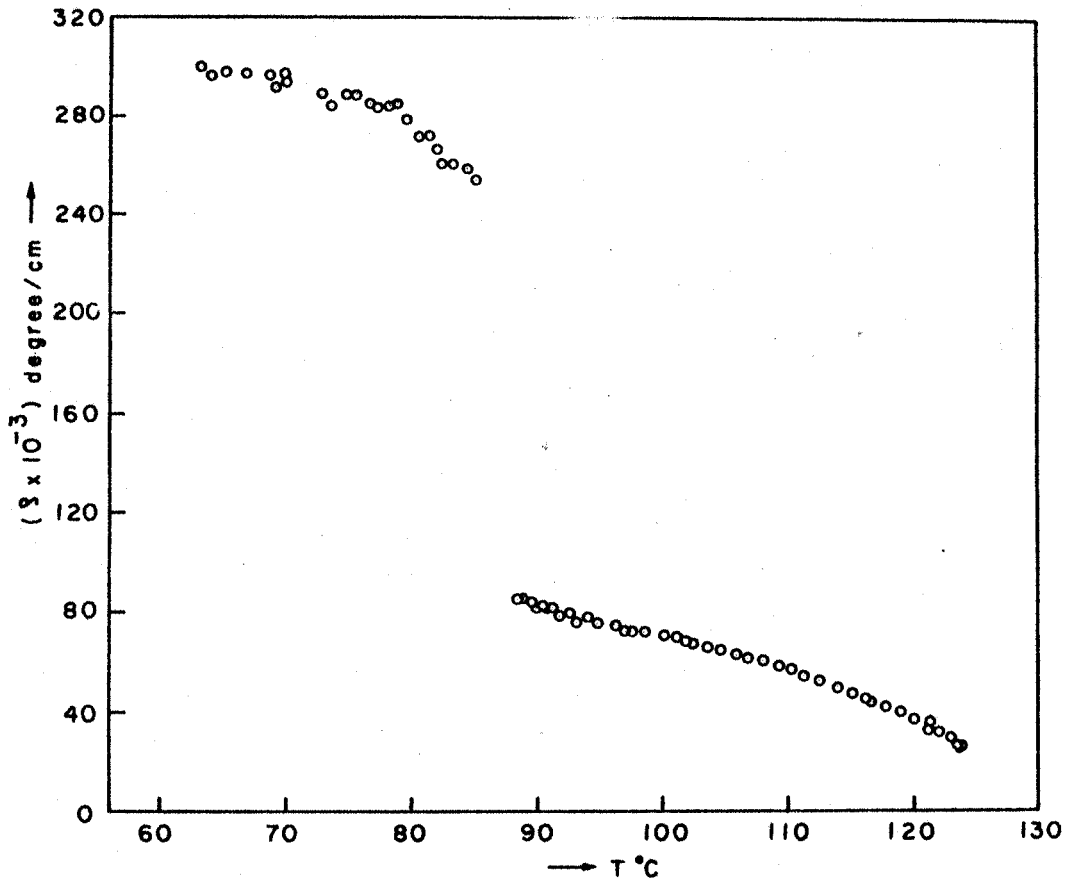
The optical rotatory power as a function of temperature was measured for both mixtures

using a standard polarimetric arrangement (Model No. 103071, Winkel Zeiss, Germany) and a sodium lamp ( $\lambda = 0.5895 \mu\text{a}$ ). The sample temperature was maintained by an electrically controlled heater and measured to  $\pm 0.1^\circ\text{C}$  by means of a previously calibrated constantan-chromel thermocouple. The details regarding the polarimeter, sample heater and the calibration of the thermocouple are described in Chapter 1. Thin films of the sample were prepared between glass plates having surface flatness of the order of  $\lambda/5$ . The sample thicknesses were kept uniform by using mylar spacers of 0.25 mil ( $\approx 6.4 \mu\text{m}$ ) thickness. In every experiment the actual sample thickness was found by measuring the thicknesses at an air gap which is deliberately introduced in the sample. These were measured by the channelled spectrum technique to an accuracy of  $\pm 2\%$ . The measurements in the, TN and TSC phases were carried out on plane texture samples. In the TN phase, well aligned plane texture films were easily obtained by the usual method of mechanical displacement of the upper glass plate. In the TSC phase, this method did not work satisfactorily; an aligned film was

obtained only on slow cooling of a plane texture TN film and the alignment was as perfect as in the TN phase. Therefore the uncertainty in the measurement of  $\gamma$  was somewhat larger for the TSC phase ( $\pm 3\%$  as compared with  $\pm 0.5\%$  for the TN phase). At the TSC-TN transition temperature the sample alignment deteriorates. In cases where the sample splits into multidomains, the experiment had to be repeated. At the TN-TSC transition temperature the mixtures showed an almost abrupt jump in  $\gamma$  unlike the behaviour of DOBCP + cholesteryl cinnamate mixture (figure 1). The experimental data are given in figures 3 and 4. The sign of the optical rotation is negative in all cases.

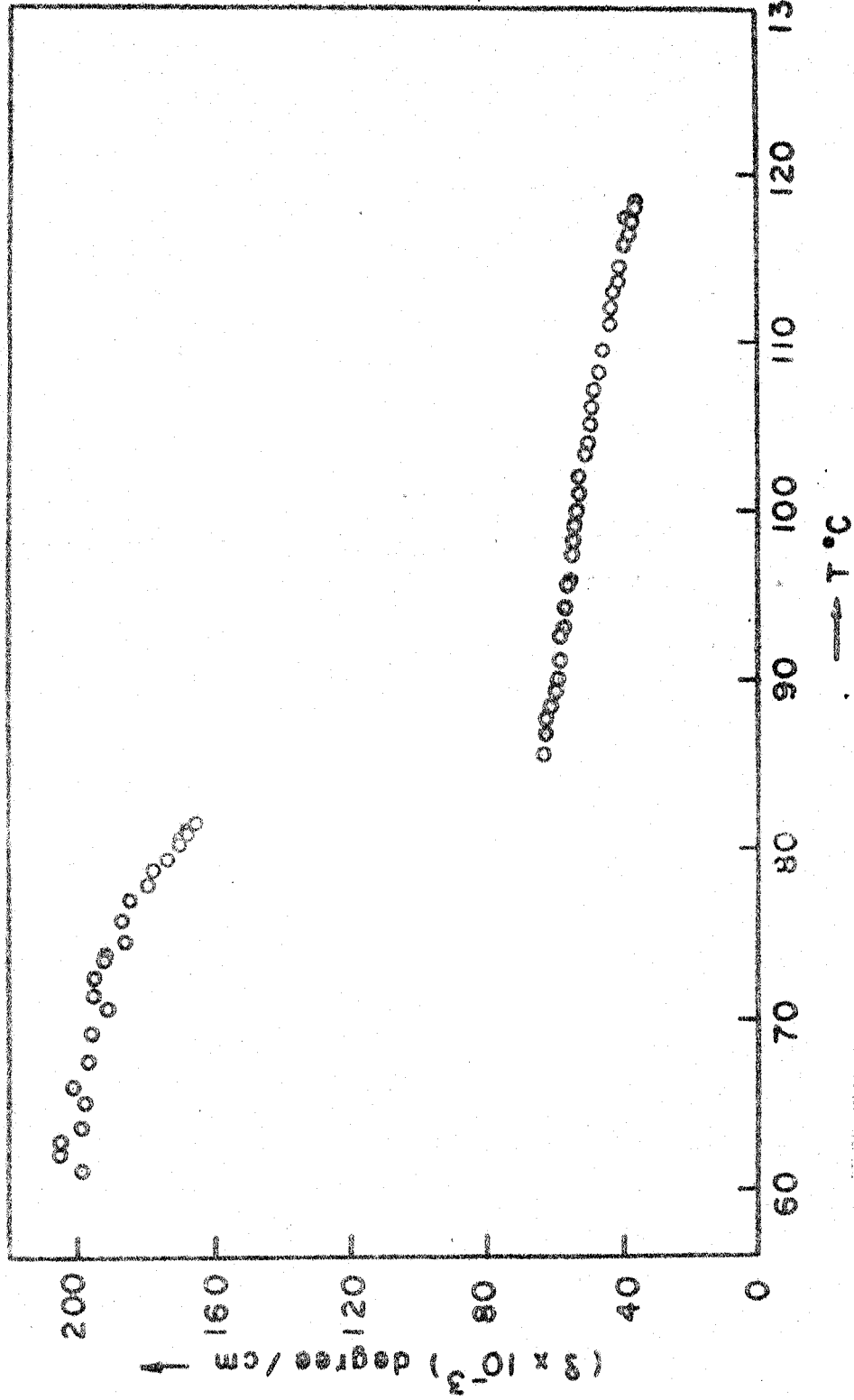
### Pitch

The pitch values of these mixtures lie in the infrared region. Therefore it is not possible to determine it by the usual light transmission or reflection experiments. Ferguson (1966) has given a 'oblique reflection' method in which by properly aligning the sample one can measure high pitch values with visible light. For a cholesteric sample with



10 % OF Ch.B IN A MIXTURE OF Ch.B & HQAB

Figure 3: Optical rotatory power as a function of temperature.



15% OF Ch.B IN A MIXTURE OF Ch.B & HOAB

Figure 4: Optical rotatory power as a function of temperature.

the helix aligned approximately parallel to the substrate the formula for P can be worked out as follows. Figure 5 depicts the reflections from cholesteric layers in this geometry. In cholesterics, if P is the pitch then P/2 is the periodicity along the helix. From Figure 5 one has

$$\varphi_B = \frac{\varphi_r' + \varphi_i'}{2}$$

i.e.,

$$\varphi_B = \frac{1}{2} \sin^{-1} \left( \frac{\sin \varphi_r}{\mu} \right) + \frac{1}{2} \sin^{-1} \left( \frac{\sin \varphi_i}{\mu} \right)$$

i.e.,

$$\begin{aligned} P \sin \varphi_B &= P \sin \frac{1}{2} \left[ \sin^{-1} \left( \frac{\sin \varphi_r}{\mu} \right) + \sin^{-1} \left( \frac{\sin \varphi_i}{\mu} \right) \right] \\ &= \frac{\lambda}{\mu} \end{aligned}$$

Therefore

$$P = \frac{\lambda}{\mu \sin \frac{1}{2} \left[ \sin^{-1} \left( \frac{\sin \varphi_r}{\mu} \right) + \sin^{-1} \left( \frac{\sin \varphi_i}{\mu} \right) \right]} \quad (1)$$



where

$\varphi_i$  = angle of incidence

$\varphi_r$  = angle of reflection

$\mu$  = average refractive index of the  
cholesteric medium

$\lambda$  = wavelength of light in vacuum.

The sample was prepared by sandwiching between two glass plates. The glass plates were thoroughly cleaned to remove grease and dust particles and the lower plate was coated with aluminium to make it highly reflecting. The alignment with helical axes approximately parallel to the substrate were obtained by slow cooling from the isotropic phase. A heater was constructed to control the sample temperature with provision to make reflection studies. The glass plates containing the sample were mounted on a solid copper cylinder which could be fixed inside the heater. The front side of the heater was covered with a glass window. This enabled to

isolate the sample thermally from outside without obstructing the light rays that are incident at large oblique angles. The temperature of the sample was measured by a constantan-chromel thermocouple. The experimental set up to measure  $\varphi_i$  and  $\varphi_r$  are shown in figure 6, It consisted of a spectrometer in which the angles could be measured to an accuracy of 1 minute. The sample film was positioned in the vertical plane inside the heater which in turn was placed on the turn table of the spectrometer. Light from a sodium lamp ( $\lambda = 0.5893 \mu\text{m}$ ) was rendered parallel by the collimator and was made to fall on the sample and the reflected light was viewed in the telescope. The position of the telescope and that of the turn table, was adjusted to get the reflected ray in the centre of the field of view of the telescope. The angle between the collimator and the normal to the sample film gives  $\varphi_i$  and the angle between the normal to the sample film and the telescope gives the angle of reflection  $\varphi_r$ . The angles  $\varphi_i$  and  $\varphi_r$  were measured at various temperatures. The sharpness of the

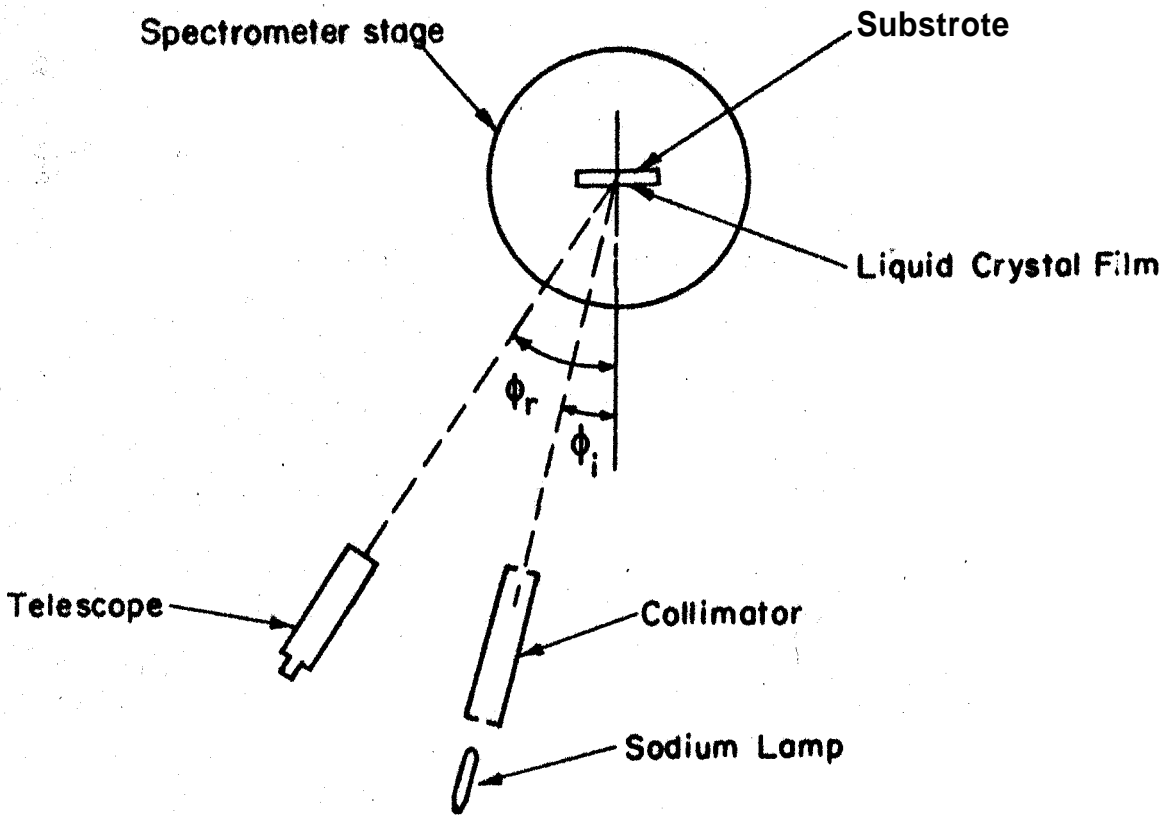


**Figure 6:** Experimental geometry to determine  $\phi_i$  and  $\phi_r$  .

reflection depends on the birefringence of the sample and on the alignment, Also it depends on sample thickness. It was found that samples of thickness  $10\ \mu\text{m}$  in the TN phase and  $5\ \mu\text{m}$  in the TSC phase are suitable for the experiments. In HOAB + CB mixtures, the reflections were not very sharp but still measurements were possible both in the IN and TSC phase except in the region close to TSC-TN transition temperature in the TSC phase. Using equation (1) the P values were calculated for various temperatures both in the TN and TSC phases. The experimental results are presented in figures 7 and 8. It shows that the pitch is dependent on temperature in the TN phase and independent of temperature in the TSC phase.

The pitch in the TN phase was also measured by recording the transmission through a plane texture film using a Leitz double beam infrared spectrophotometer (Model 081). Here the samples were sandwiched between two calcium fluoride discs each of diameter 30 mm and thickness 4 mm. The arrangement to heat the sample and to measure the temperature was similar to that used in the

**Figure 7: Pitch as a function of temperature for a mixture of 0.9 HOAB + 0.1 GB. Circles represent the data obtained by the oblique reflection method and squares by the infrared transmission method.**



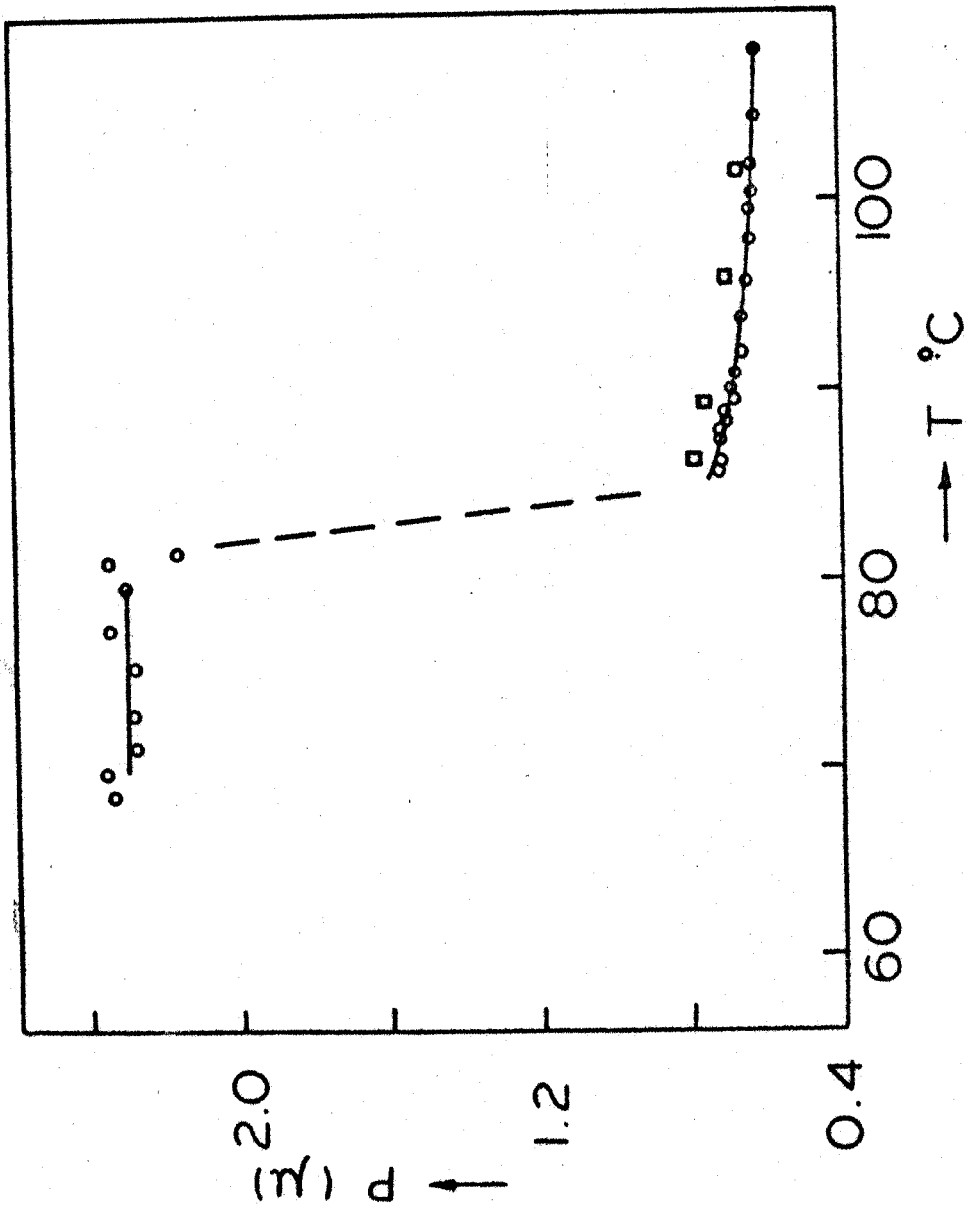


**Figure 8: Pitch as a function of temperature for a mixture of 0.85 HOAB + 0.15 CB. Circles represent the data obtained by the oblique reflection method and squares by the infrared transmission method.**

measurement of  $\xi$  as a function of temperature. Infrared rays from a Nernst lamp were passed through the sample (maintained at a temperature) and the transmitted intensity was recorded as a function of wavelength. In the transmission spectrum a dip in the intensity corresponding to the reflection band  $\lambda_0$  was observed. The pitch was calculated from the relation  $\lambda_0 = \mu P$  where  $\mu$  was assumed to be the average of  $\mu_1$  and  $\mu_2$ , the principal indices of the layer at the wavelength  $\lambda_0$ . (These were obtained from Drude's dispersive formula using the values of  $\mu_1$  and  $\mu_2$  corresponding to optical wavelength.) The procedure was repeated at various sample temperatures. This technique yields a more precise estimate of the pitch. These experimental values are also presented in figures 7 and 8. These values are slightly higher than those obtained from the oblique reflection technique.

### Birefringence

The birefringence  $\Delta\mu$  of pure HOAB was determined in the nematic and smectic C phases by

measuring the phase retardation (in a sample of known thickness) using a Babinet compensator. The sample was taken between two glass plates (of dimensions 11 mm square and 2 mm thickness) having surface flatness of the order of  $\lambda/10$ . The surfaces were cleaned thoroughly and then coated with a very thin aluminium layer. This eliminates surface flaws but transmits light. The thickness of the sample was kept uniform over the whole area by using a mylar spacer of nominal thickness of 38  $\mu\text{m}$ . The actual thickness was measured by the channelled spectrum technique. Again a heater was constructed similar to the one described for the determination of  $\delta$  but; with much smaller dimensions (diameter of the outer cylinder  $\approx 30$  mm) to enable it to fit into the space between the pole pieces of the magnet. The temperature of the sample was sensed by a constantan-chromel thermocouple calibrated in the usual way. The sample was aligned by a magnetic field of strength 7.5 K Gauss and all measurements were made in the presence of the field after the specimen had remained in it for nearly 2 hours.

The experiment consisted of sending a parallel beam of light from a sodium lamp ( $\lambda = 0.5893 \mu\text{m}$ ) through a polariser, that sample and a Babinet compensator. At each temperature the number of fringes  $m$  crossing the reference line in the field of view of the Babinet compensator was noted. Then  $\Delta\mu$  of the medium was calculated from the relation

$$\Delta\mu = \frac{m\lambda}{t}$$

where

$t$  = sample thickness

$\lambda$  = wavelength of light in vacuum.

The experimental values of  $\Delta\mu$  in the nematic and smectic C phases are presented in Figure 9. It shows that  $\Delta\mu$  has a discontinuity at the nematic-smectic C transition and also that  $\Delta\mu$  depends strongly on temperature in the nematic phase as compared to smectic C phase.

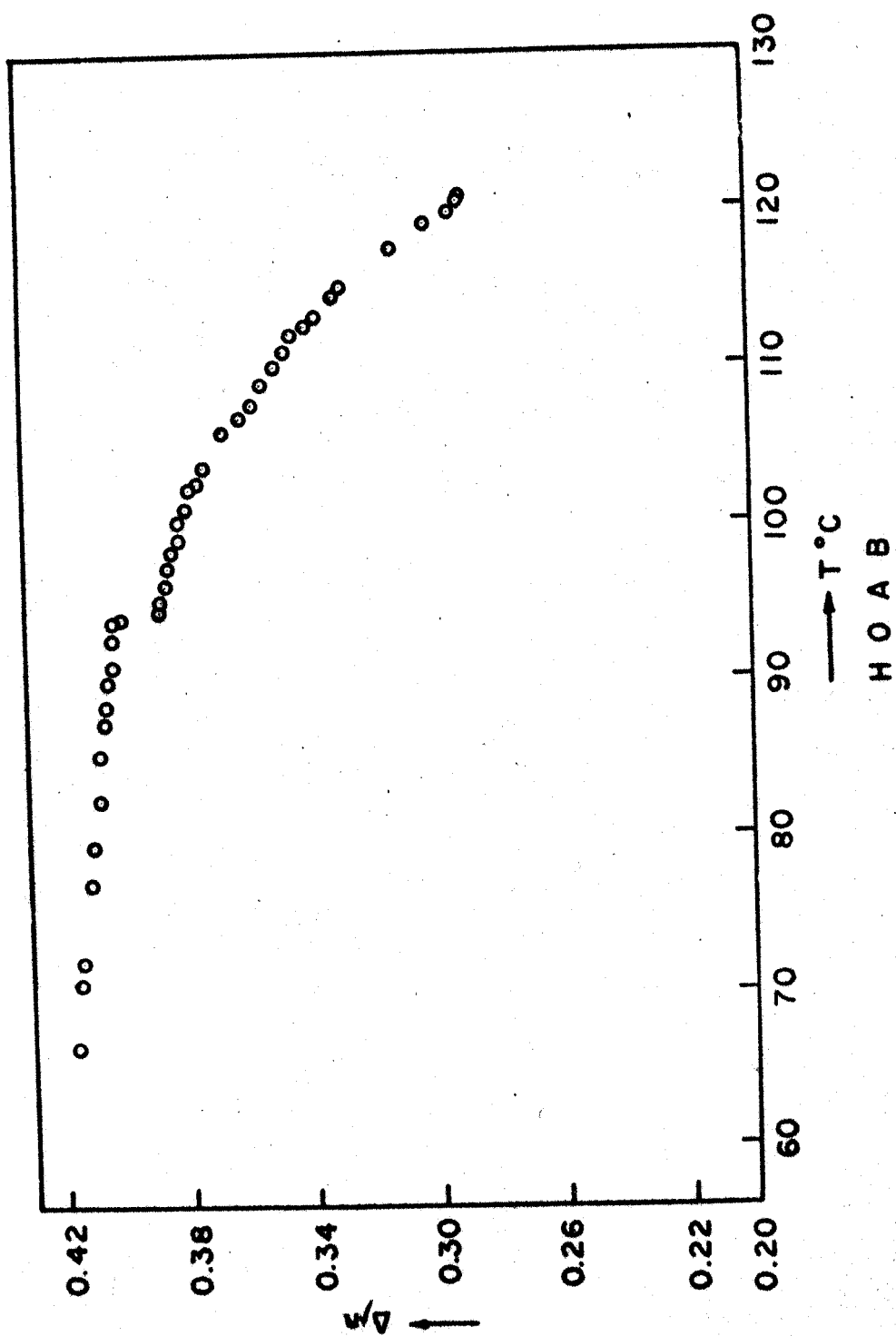


Figure 9: Birefringence versus temperature for pure HOAB oriented in a magnetic field.

### 3. Comparison with theory

Equations for the two wave vectors for normal waves as given by the rigorous theory were used to calculate the optical rotatory power from a knowledge of  $P$  and  $A \mu$ .

From equation (30) of Chapter III, the two wave vectors are

$$k_2, k_1 = [K_m^2 + q_0^2 \pm (4K_m^2 q_0^2 + B^2 K^4)^{\frac{1}{2}}]^{\frac{1}{2}}$$

$$= K_m \left[ 1 + \frac{q_0^2}{K_m^2} \pm \left( 4 \frac{q_0^2}{K_m^2} + \frac{B^2 K^4}{K_m^4} \right)^{\frac{1}{2}} \right]^{\frac{1}{2}}$$

Here

$$\frac{q_0}{K_m} = \frac{2\pi \lambda}{P(\epsilon)^{\frac{1}{2}} 2\pi} = \frac{\lambda}{P(\epsilon)^{\frac{1}{2}}} = \frac{\lambda}{P[\frac{1}{2}(\mu_1^2 + \mu_2^2)^{\frac{1}{2}}]} = \lambda' \text{ (say)}$$

..(2)

$$\frac{BK^2}{K_m^2} = \frac{B}{\epsilon} = \frac{\epsilon_a - \epsilon_b}{2 \frac{(\epsilon_a + \epsilon_b)}{2}} = \frac{\mu_1^2 - \mu_2^2}{\mu_1 - \mu_2} = \alpha \text{ (say)} \quad (3)$$

$$\text{i.e., } k_2, k_1 = K_m [1 + \lambda'^2 \pm (4 \lambda'^2 + \alpha^2)^{\frac{1}{2}}]^{\frac{1}{2}}$$

Putting

$$m_1 = \frac{k_1}{K_m} = [1 + \lambda'^2 - (4\lambda'^2 + \alpha^2)^{\frac{1}{2}}]^{\frac{1}{2}} \quad (4)$$

$$m_2 = \frac{k_2}{K_m} = [1 + \lambda'^2 + (4\lambda'^2 + \alpha^2)^{\frac{1}{2}}]^{\frac{1}{2}} \quad (5)$$

The optical rotatory power

$$\begin{aligned} \rho &= \frac{K_1 - K_2}{2} = \frac{(k_1 + q_0) - (k_2 - q_0)}{2} = \frac{k_1 - k_2}{2} + q_0 \\ &= \frac{K_m}{2} (m_1 - m_2) + q_0 \\ &= \frac{q_0}{2\lambda'} (m_1 - m_2) + q_0 = \frac{\pi}{P\lambda'} (m_1 - m_2) + \frac{2\pi}{P} \end{aligned}$$

i. e.,

$$\rho = \frac{\pi}{P} \left[ 2 + \frac{(m_1 - m_2)}{\lambda'} \right] \quad (6)$$

Using equations (2) to (6) along with the observed values of pitch one can calculate the rotatory power provided the birefringence of the

mixture is known. The birefringence of CB was assumed to be 0.05 and using the birefringence of HOAB, the birefringence of the mixture was obtained by a simple additivity law. The rotatory power  $\rho$  in the TN phase was calculated for the 0.9 HOAB + 0.1 CB mixture. The calculated values together with the experimental values are given in table 2. From this, one finds that the theoretical values are nearly twice the experimental values. This indicates that the molecules are probably not normal to the helical axis (as in the classical cholesteric) but tilted resulting in a reduction of the effective birefringence for this direction of propagation. Chatelain and Cano have also come to similar conclusions while interpreting the observed optical rotatory power in a p-azoxy-phenetale cholesteryl benzoate mixture. X-ray studies were undertaken to verify this conclusion.

#### 4. X-ray Studies

X-ray diffraction photographs of randomly oriented samples of pure HOAB and of the 0.9 HOAB + 0.1 CB mixture were taken at different temperatures using Nickel filtered  $\text{CuK}\alpha$  radiation ( $1.542 \text{ \AA}$ ) from a Raymax (England) X-ray unit. The specimen was taken in the form of a free film of about 2 mm

Table 2

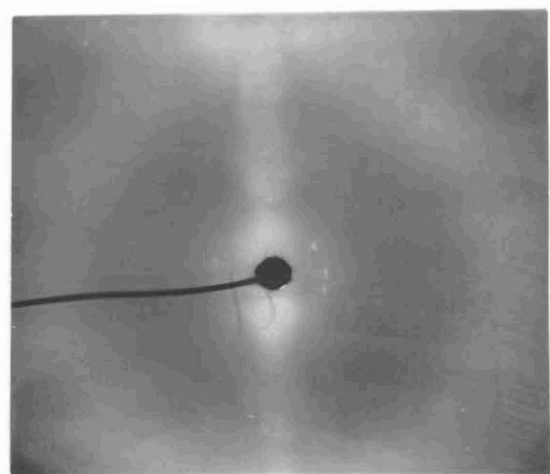
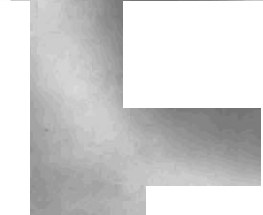
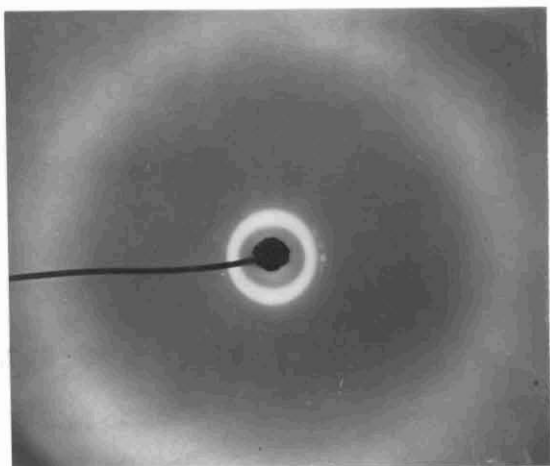
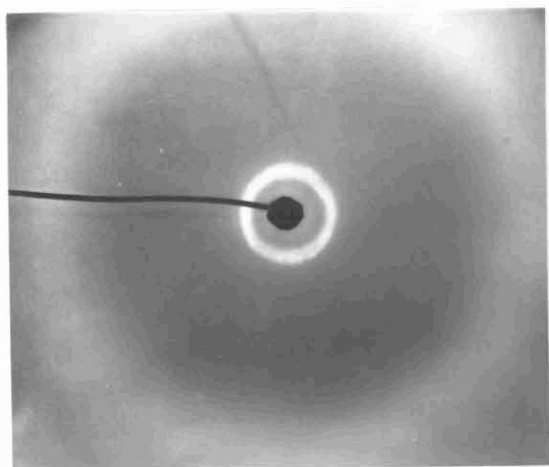
$(T_1 - T)^\circ \text{C}$	Rotatory power ( $\beta$ ) $\times 10^{-3}$ deg $\text{cm}^{-1}$		
	Experimental	Calculated with $\varphi_t = 90^\circ$	Calculated with $\varphi_t = 39^\circ$
4	33.0	78.50	18.67
8	42.2	92.09	22.01
12	50.5	106.50	24.67
16	58.0	118.20	26.88
20	64.0	130.41	28.96
24	69.5	139.12	30.21
28	72.4	145.96	31.47
32	78.0	-	-

$\beta$  values in the TN phase for 10% CB + 90% HOAB mixture at temperatures relative to the isotropic temperature  $T_i$ .

in diameter on a loop of wire. For this geometry a different type of heater is required. This was constructed in the usual way but with facility to place the wire loop at the centre. Thin mylar windows were used to isolate the sample thermally from external disturbances. The sample temperature was sensed by a constantan-chromel thermocouple and the e.m.f. developed in it was measured by a Philips microvoltmeter. The diffraction photographs are shown in figure 10. In all cases, with the exception of the one taken for the isotropic phase, there occurs a relatively intense inner ring and a faint outer ring. For the smectic C phase of pure HOAB and the TSC phase of the mixture, the inner ring is quite sharp as would be expected of a smectic layered structure. On the other hand, for the nematic phase of HOAB and the Ti<sup>?</sup> phase of the mixture, the inner ring is more diffuse. Still the inner ring is of greater intensity compared to the outer ring in both cases, characteristic of a cybotactic structure.

In every case, the diameter of the inner ring was measured using a comparator. The tilt

**Figure 10: X-ray diffraction patterns for unaligned samples. Pure HOAB in the smectic C phase (top left) and in the nematic phase (bottom left). The 0.9 HOAB + 0.1 CB mixture in the twisted smectic C phase (top right), twisted nematic phase (middle right) and isotropic phase (bottom right). The spots in the photographs on the right are due to the sample holder.**



angle  $\varphi_t$  (defined with respect to layer normal) is calculated from the relations

$$\left. \begin{aligned} \varphi_t &= \cos^{-1} (d/l) \\ d &= \frac{\lambda}{2 \sin \theta} \\ \theta &= \frac{1}{2} \tan^{-1} \left[ \frac{S}{2R} \right] \end{aligned} \right\} \quad (7)$$

where  $\lambda = 1.542 \text{ \AA}$  is the wavelength of X-rays,  $l$  = length of the molecule and was assumed to be  $33 \text{ \AA}$  for HOAB (Chistyakov and Chaikowsky 1969),  $R$  = distance between the sample and the photographic film\*

The tilt angles calculated in the different phases are given below.

Smectic C phase of pure HOAB	=	44°
Nematic phase of pure HOAB	=	41°
TSC phase of 0.9 HOAB + 0.1 CB	=	41.5°
TN phase of 0.9 HOAB + 0.1 CB	=	39° .

It was found that the tilt angles in all the phases are practically independent of temperature.

A photograph taken in the isotropic phase for the mixture shows a very weak and diffuse inner ring indicating traces of cybotactic nature.

## 5. Discussion

On the basis of the evidence obtained from X-ray studies, the theoretical rotatory power of the TN phase was recalculated taking the molecules to be tilted at  $39^\circ$  to the helical axis.

The effective layer refractive index  $\mu_e$  for an electric vector polarised in the plane of the tilt for light propagating normal to the layer is given by

$$\frac{1}{\mu_e^2} = \frac{\cos^2 \varphi_t}{\mu_1^2} + \frac{\sin^2 \varphi_t}{\mu_2^2} \quad (8)$$

where  $\varphi_t$  is the tilt angle with respect to the helical axis. Here  $(\mu_e - \mu_1)$  gives the layer birefringence. It was assumed that  $\mu_1 = 1.55$  which is the approximate value of the ordinary index for p-azoxyanisole and other similar compounds. The calculated values of  $\zeta$  are given in table 2 (page 107).

A similar calculation is carried out for the twisted smectic C, taking the tilt angle to be  $41.5^\circ$  and  $\rho$  calculated at a few temperatures are given in table 3. The experimental values of  $\rho$  for TN phase and TSC phase are also presented in the above tables for comparison. Surprisingly, the theoretical values turn out to be about half of the experimental values in both the TN and TSC phases. One reason for the higher effective optical rotation may be the tendency of the molecules at the boundary to align parallel to the glass surfaces, thus increasing the effective layer birefringence of the medium at the boundary. (see Figure 11) There may also be changes in the twist between successive layers close to the boundary. In order to investigate this, measurement of  $\rho$  on samples of different thicknesses were undertaken. The results are given in Figure 12. It indicates that the rotatory power decreases with increasing thickness suggesting a boundary layer effect. This may partly account for the discrepancy between the experimental and calculated values. A reliable estimate of the contribution of the boundary layer to the rotatory power is difficult as there are

Table 3

$(T_{SN}-T)^{\circ}C$	Rotatory power ( $\rho$ ) $\times 10^{-3}$ deg.cm $^{-1}$	
	Experimental	Calculated with $\phi_t = 41.5^{\circ}$
4	258	131.72
8	276	133.16
12	287	134.70
16	290	136.04
20	297	137.17
24	299	138.10

$\rho$  values in the TSC phase for 10% CB + 90% HOAB mixture at temperatures away from  $T_{SN}$ , the TSC to TN transition point.

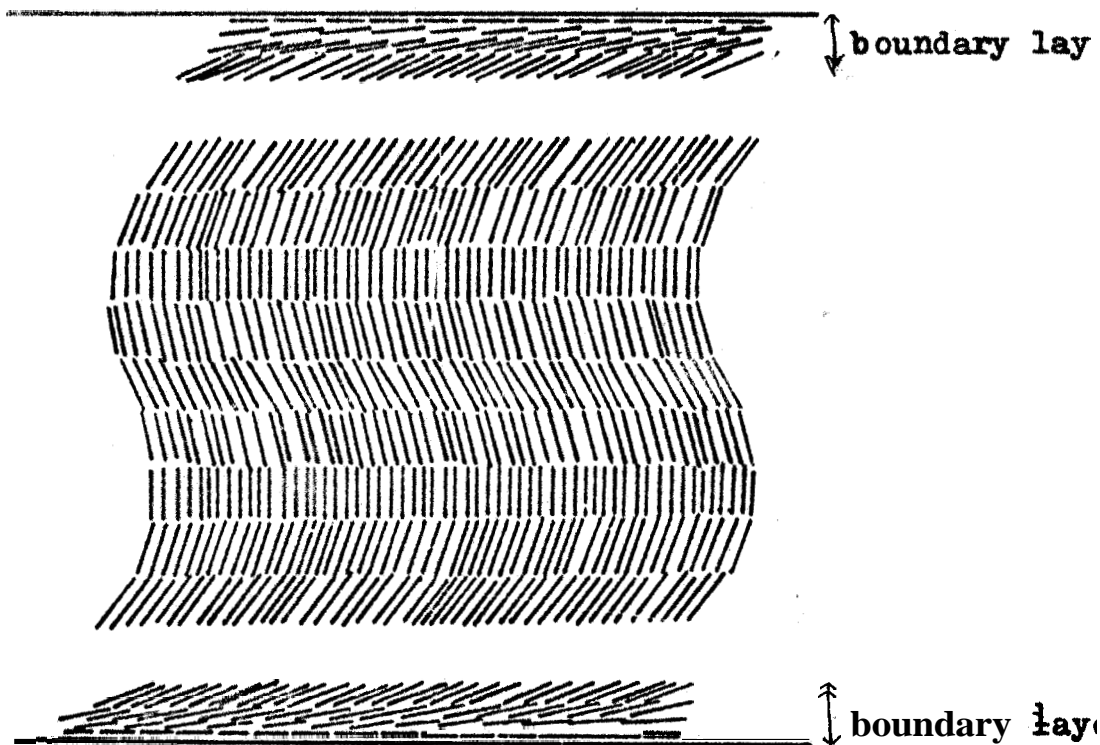
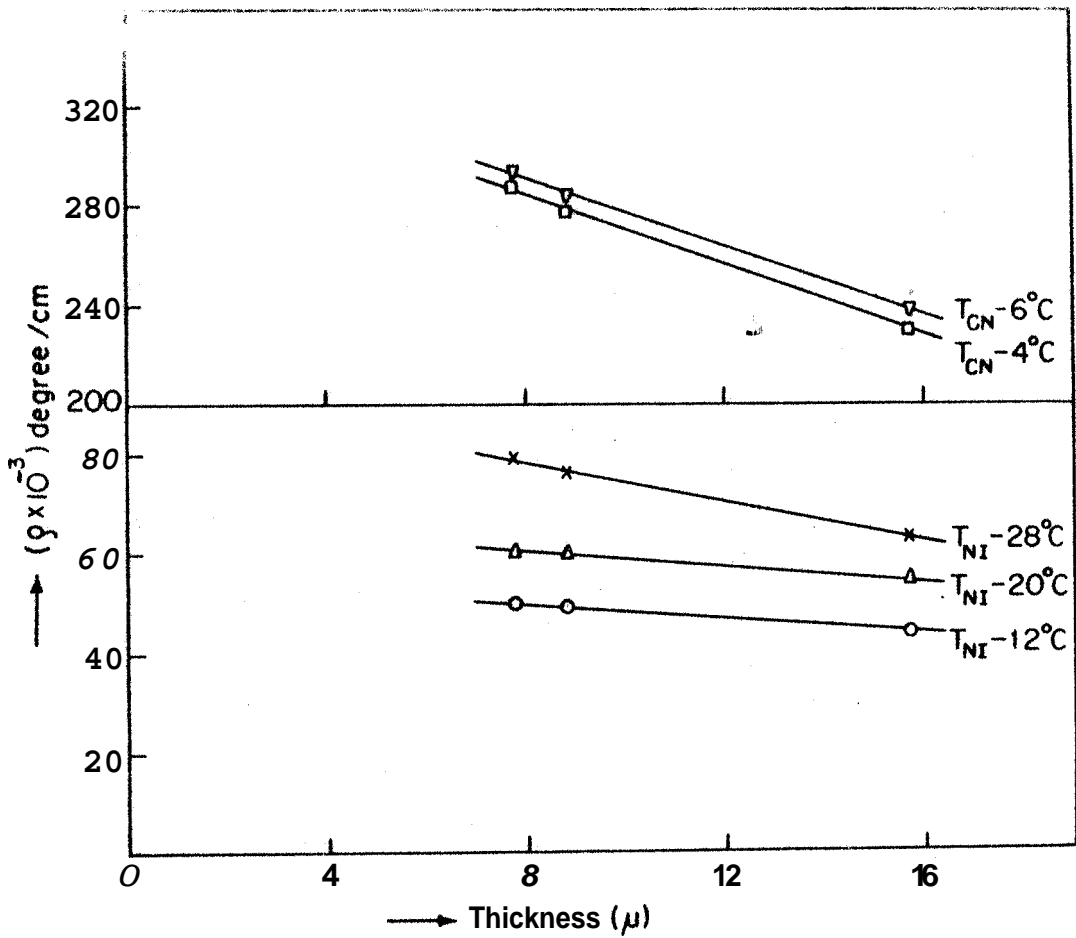


**Figure 11:** Schematic representation of change in tilt angle of twisted smectic C near the walls.

**Figure 12:** Optical rotatory power as a function of thickness for the 0.9 HOAB + 0.1 CB mixture at various temperatures.  $T_{NI}$  represents the nematic-isotropic transition temperature and  $T_{CN}$  represents the TSC-TN transition temperature.



likely to be changes in the tilt as well as the pitch of the structure.

Moreover in the calculations of the layer birefringence of the mixture, the simple additivity law was used. Actually, dissolving CB in HOAB changes the transition temperatures and also the range of the liquid crystal phases. Thus there are likely to be appreciable changes of order parameter which in turn would alter the layer birefringence of the mixture. Since  $\xi$  varies as the square of the birefringence this contribution may be partly responsible for the discrepancy between theory and experiment.

Despite this difficulty in understanding the difference between calculation and experiment, the X-ray results together with the optical evidence presented in this chapter appear to show fairly conclusively that the twisted-nematic phase of the mixture has a structure quite different from the usual cholesteric in that the molecules are not normal but tilted with respect to the helical axis.

References

- Arora, S.L., Fergason, J.L. and Saupe, A. 1970  
Mol. Cryst. Liquid Cryst. 10, 243.
- Berreman, D.W. 1973 Mol.Cryst.Liquid Cryst. 22, 175.  
[Berreman and Scheffer have considered the problem  
of oblique reflection from a plane texture  
cholesteric liquid crystal. Ref: Berreman, D.W.  
and Scheffer, T.J. 1970 Phys.Rev.Lett. 25, 577.]
- Brunet, M. 1975 3. de Physique 01-321.
- Brunent-Germain, M. 1970 Acta Cryst. A26, 595.
- Cano, R. and Chatelain, P. 1964 C.R.Acad.Sci.  
259, 352.
- Chistyakov, I.G. and Chaikowsky, W.M. 1969  
Mol. Cryst. Liquid Cryst. 7, 269.
- Fergason, J.L. 1966 Mol. Crystals, 1, 309.
- Helfrich, W. and Oh, G.S. 1971 Mol. Cryst. Liquid  
Cryst. 14, 289.
- Leclerq, M.L., Billard, J. and Jacques, J. 1969  
Mol. Cryst. Liquid Cryst. 8, 367.
- Saupe, A. 1969 Mol.Cryst. Liquid Cryst. 7, 59.
- Suresh, K.A. and Chandrasekhar, S. 1976 Mol. Cryst.  
Liquid Cryst. (in press).
- Taylor, T.R., Fergason, J.L. and Arora, S.L. 1970  
Phys. Rev. Lett. 24, 359.